Available online at www.sciencedirect.com
ScienceDirect
Bioelectrochemistry 69 (2006) 49–57
Bioelectrochemistry
www.elsevier.com/locate/bioelechem

Dielectric spectroscopy of *Anabaena 7120* protoplast suspensions

Kongshuang Zhao [a,*], Wei Bai [a], Hualing Mi [b]

[a] *Department of Chemistry, Beijing Normal University, 100875, Beijing, China*
[b] *National Laboratory of Plant Molecular Genetics, Institute of Plant Physiology & Ecology, Chinese Academy of Sciences, Shanghai, China*

Received 16 June 2005; received in revised form 19 October 2005; accepted 31 October 2005
Available online 20 January 2006

Abstract

The dielectric spectroscopy of *Anabaena 7120* protoplast suspensions has been investigated over the frequency range of 40 Hz–110 MHz. The protoplast suspensions showed a complicated dielectric dispersion consisting of at least four distinct sub-dispersions with the increasing frequencies due to the Maxwell–Wagner interfacial polarization. The double-shell model, in which an equivalent shell of thylakoid was assumed inside the cytoplasm, was adopted to describe the special morphology of the protoplast. Under the assumption that the conductivity of plasmalemma was negligible and the conductivity of the equivalent shell was 0.1 μS/cm, we attempted to estimate the dielectric properties of various protoplast components by fitting theoretical curve to experimental data. The relative permittivity of the plasmalemma ε_{mem} was estimated to be 6.5±0.5, and the permittivity of the equivalent shell of thylakoid ε_{thy} was estimated to be about 3.2±0.2. The permittivity ε_{cyt} and conductivity κ_{cyt} of the cytoplasm were estimated to be 60 and 0.88±0.11 mS/cm, respectively. The permittivity ε_{nuc} and conductivity κ_{nuc} of the nucleoplasmic region were determined to be 100 and 0.13±0.02 mS/cm, respectively.

Keywords: Dielectric spectroscopy; *Anabaena*; Protoplast; Thylakoid

1. Introduction

Anabaena 7120 is a heterocystous cyanobacterium. It is an ideal model system to study photosynthesis, cell differentiation, pattern formation and cellular interaction [1,2]. The marked characteristic for *Anabaena* cells is that they have an inner system called thylakoid, which are the sites of photosynthetic and respiratory electron transport [3,4]. To study the mechanism, the usual approach is the isolation of thylakiod from cyanobacteria and then photoelectric studies of transmembrane charge transfer reactions of pigments and proteins located on them [5,6]. Recently a few researchers studied the relationship between the photosynthesis and the dielectric response of the proteins located on the thylakoids [7–9]. These studies indicated that dielectric properties of the thylakoid played an important role in the process of photosynthesis.

Dielectric analysis of cell suspensions is a rather effective technique providing the dielectric properties of cellular components, such as the plasmalemma and the cytoplasm, etc. [10–20]. Since Fricke [21] firstly applied dielectric spectroscopy to study the erythrocyte and predicted the thickness and the capacitance of erythrocyte membrane which is consistent with the result later determined by the electronic microscope, the dielectric spectroscopy, as a non-invasive method for exploring structure–function relationships, has frequently been applied to various biological cells and tissues. As far as dielectric properties of plant protoplasts are concerned, many studies have been carried out by using different techniques, including the electrorotation method [22–26], and the dielectrophoresis method [27], and dielectric spectroscopy [28]. Because of their highly complex membranous apparatus, however, cyanobacterium cells have been not studied so far. In the present paper, the authors attempted to take use of the technique of dielectric spectroscopy to study *Anabaena 7120* protoplast in order to provide the dielectric properties of its components and to give a certain interpretation for its complicated dielectric behavior.

* Corresponding author. Tel.: +86 10 58808283.
E-mail address: zhaoks@bnu.edu.cn (K. Zhao).

1567-5394/$ - see front matter © 2006 Elsevier B.V. All rights reserved.
doi:10.1016/j.bioelechem.2005.10.004

2. Materials and methods

2.1. Preparation of protoplast suspensions

Anabaena 7120 cells were cultivated at 30 °C under constant illumination in BG-11 medium [29]. The cells were harvested by centrifugation for 10 min at 5000 ×*g*. The cell pellets were washed with buffer A, which contained 0.4 M sucrose, 1 mM EDTA and 30 mM HEPES, pH 7.0, and were centrifuged again for 10min at 5000 ×*g*. Then the cell pellets were resuspended in buffer A plus 1.5 mg/ml lysozyme and were incubated at 30 °C for 2–3 h. After incubation, the cells became the separate spherical protoplasts in the absence of mechanical support of cell wall. Finally the protoplasts were centrifuged for 10 min at 5000 ×*g* and the pellets were collected. The collected protoplast pellets were immediately resuspended in a certain amount of distilled water. Then this protoplast suspension was separated equally into three samples, and finally each sample was diluted successively with the distilled water to prepare the protoplast suspensions with different concentrations, which were subjected to dielectric measurement. In this way, we obtained three sets of protoplast suspensions with different concentrations, and each concentration has three parallel samples with the same concentration. The mean radius was 3.0 μm measured by using optical microscope.

2.2. Dielectric measurements

The equivalent parallel capacitances and conductances of protoplast suspensions were measured by computer-controlled Impedance Analyzers (model 4294 A, Agilent Technologies) equipped with a 16047 E Spring Clip fixture over the frequency range from 40 Hz to 110 MHz. The measuring cell was a parallel plate capacitor consisting of two platinized platinum plates and a lucite spacer, cell constant and sample space being 0.02 pF and 200 μl, respectively. The details of the measuring cell were described elsewhere [30]. The data were corrected for residual inductance and stray capacitance arising from the measuring cell and its lead wire according to the method described by K. Asami et al. [31]. The correction was, however, somewhat insufficient at higher frequencies. It can been seen that an unexpected slight increase in conductivity still remained, which might be due to some instrumental errors or the orientation polarization of water and biological macromolecular. All measurements were performed at 20±1 °C. Simultaneously, after the measurements the suspensions were centrifuged immediately and the supernatants were measured to determine the permittivity (ε_a) and conductivity (κ_a) of the suspending medium. The measurement of each sample was completed in about 3 s.

2.3. Correction for electrode polarization artifacts

At lower frequencies, a marked electrode polarization effect dominates, owing to the counterion accumulation at the electrode-aqueous phase interface. The electrode polarization impedance is a complex quantity, including the real and imaginary part, and is in series with that of protoplast suspensions. To eliminate the real and imaginary parts of the electrode polarization, we measured the impedance of the solution without cell (i.e., the supernatant obtained by centrifuging protoplast suspensions), and decomposed that into a complex impedance element in series with a simple solution conductance and parallel with cell capacitance and then subtracted the complex impedance from the raw data before performing theoretical analysis.

3. Electric model of the spherical protoplast

3.1. Description of the model based on its morphology

The removal of the cell wall makes us easily to model the spherical protoplast. Fig. 1(a) shows the electron micrograph of the protoplasts isolated from *Anabaena 7120* that were subjected to dielectric measurements. It shows that the peripheral region of cytoplasm contains many membranous photosynthetic apparatus in the protoplast. In unicellular forms they commonly consist of a few membrane layers, which extend in concentric sheets beneath the plasmalemma and surround the central nucleoplasmic region. The basis structure of the membranes resembles a flattened sac and is known as the thylakoid. The appressed membranes of the thylakoid may occasionally or partially separate displaying the inner cavity of the thylakoid sac. As a species of prokaryotic algae, there is no nuclear envelope and few organelles in the protoplast [1].

Here the single-shell model [13] and the "double-shell" model [32] were employed to model the protoplast as depicted in Fig. 1(b) and (c). In the single-shell model, the protoplast is regarded as a conducting homogeneous sphere (corresponding to the cytoplasm ε_i^*) covered by a poorly conducting concentric shell (corresponding to the plasmalemma ε_{mem}^*, thickness, d_{mem}). Whereas in the "double-shell" model, we assumed that there was an equivalent closed spherical concentric shell inside the cytoplasm, i.e., sheets of thylakoids in the peripheral region of cytoplasm were assumed to be an equivalent homogeneous spherical shell composed of one closed sheet of thylakoid (ε_{thy}^*, thickness d_{thy} ($=2d_{mem}$, because the thylakoid can be roughly considered to be composed of two appressed membranes)), inside which there was the nucleoplasmic region (ε_{nuc}^*); and the cytoplasm between sheets of thylakoids, together with the cytoplasm between the plasmalemma and the most outer thylakoid, were unified into the cytoplasm layer (ε_{cyt}^*). Such assumption can be interpreted by means of the Maxwell–Wagner interfacial polarization theory [33–35], in which a dielectric dispersion occurs when two phases with different electric properties, such as these thylakoids and the cytoplasm, contact with each other in the external electric field. Furthermore, because the electric properties of all thylakoids are identical, and those of the cytoplasm surrounding them are also the same, so there is only one kind of interface between sheets of thylakoids and cytoplasm, which only produces a single dielectric dispersion. In this way, it is reasonable theoretically that sheets of thylakoid are assumed to be an equivalent spherical shell composed of one sheet of thylakoid.

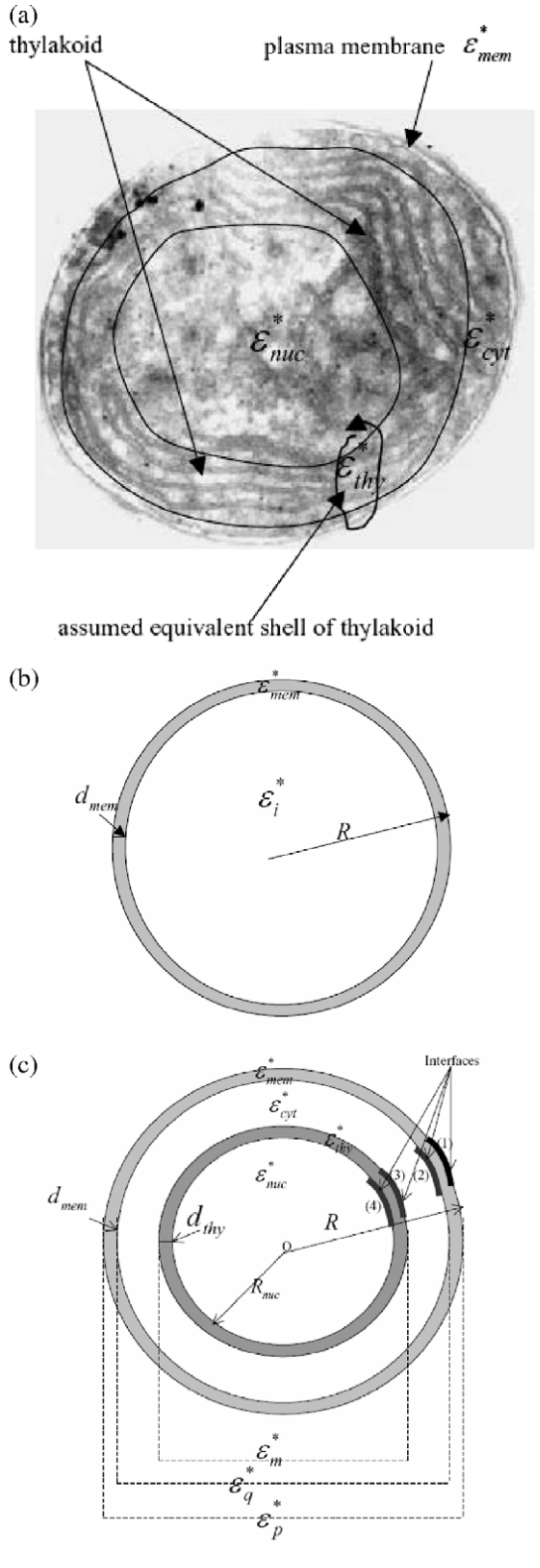

Fig. 1. (a) The electronic micrograph of the protoplast. (b) The single-shell model. (c) The double-shell model. d_{mem}: thickness of the plasmalemma (d_{mem}=7 nm), d_{thy}: thickness of the assumed equivalent spherical shell of thylakoid (d_{thy}=14 nm), R: the radius of protoplast, R_{nuc}: the radius of the nucleoplasmic region. The numbers from (1) to (4) denote four different kinds of interfaces.

3.2. Theoretical expression of the cell model

For a suspension of spherical particles uniformly dispersed in a dilute medium, the equivalent, homogeneous permittivity ε^* for the cell suspensions is given by:

$$\varepsilon^* = \varepsilon_a^* \frac{2(1-P)\varepsilon_a^* + (1+2P)\varepsilon_p^*}{(2+P)\varepsilon_a^* + (1-P)\varepsilon_p^*} \tag{1}$$

where P is the volume fraction, which is small enough to neglect the mutual polarization effect between the suspended particles, ε_a^* is the complex permittivity of the suspending medium, ε_p^* is the equivalent complex permittivity of protoplast as a whole, which can be expressed by Eq. (2). Complex permittivity ε^* is defined as $\varepsilon^*=\varepsilon-j\kappa/(\omega\varepsilon_v)$, in which ε is real permittivity, κ is conductivity, j is unit imaginary, ε_v is the permittivity of vacuum ($=8.854\times10^{-12}$ F/m), $\omega=2\pi f$, where f is frequency. It is necessary to mention that some researchers have demonstrated that Eq. (1) could be safely used up to volume fractions of 0.4, which was beyond the values in the present paper (P=0.04–0.23) [36,37]

$$\varepsilon_p^* = \varepsilon_{mem}^* \frac{2(1-v_3)\varepsilon_{mem}^* + (1+2v_3)\varepsilon_q^*}{(2+v_3)\varepsilon_{mem}^* + (1-v_3)\varepsilon_q^*} \tag{2}$$

where $v_3=(1-d_{mem}/R)^3$, ε_{mem}^* is the complex permittivity of the plasmalemma, ε_q^* is the equivalent complex permittivity of the sphere inside the plasmalemma.

$$\varepsilon_q^* = \varepsilon_{cyt}^* \frac{2(1-v_2)\varepsilon_{cyt}^* + (1+2v_2)\varepsilon_m^*}{(2+v_2)\varepsilon_{cyt}^* + (1-v_2)\varepsilon_m^*} \tag{3}$$

where $v_2=((R_{nuc}+d_{thy})/(R-d_{mem}))^3$, ε_{cyt}^* is the complex permittivity of the cytoplasm, ε_m^* the equivalent complex permittivity of the sphere consisting of the equivalent shell of thylakoid and its interior as depicted in Fig. 1(c).

$$\varepsilon_m^* = \varepsilon_{thy}^* \frac{2(1-v_1)\varepsilon_{thy}^* + (1+2v_1)\varepsilon_{nuc}^*}{(2+v_1)\varepsilon_{thy}^* + (1-v_1)\varepsilon_{nuc}^*} \tag{4}$$

where $v_1=(R_{nuc}/(R_{nuc}+d_{thy}))^3$, ε_{thy}^* is the complex permittivity of the equivalent shell of thylakoid, ε_{nuc}^* the complex permittivity of the central nucleoplasmic region.

Theoretical simulations of the dielectric spectra were based on the Eqs. (1) (2) (3) and (4). The curve fitting procedure was similar to that described elsewhere [32]. Morphological parameters and volume fraction are taken as constants in the curve fitting process. To obtain the best-fit parameters, the residuals between theoretical curves and experiment data were minimized by means of a computer.

$$\mathrm{Dev}(\varepsilon,\kappa) = \left(\sum_i (\varepsilon_{ti}-\varepsilon_{ei})^2 / \sum_i \varepsilon_{ei}^2 + \sum_i (\kappa_{ti}-\kappa_{ei})^2 / \sum_i \kappa_{ei}^2 \right)^{1/2} \tag{5}$$

where ε and κ are permittivity and conductivity of the cell suspensions, and subscripts t and e stand for theoretical and experimental values, respectively.

Volume fraction P was calculated from the equation,

$$P = \frac{2(1-\kappa_l/\kappa_a)}{2+\kappa_l/\kappa_a} \quad (6)$$

where κ_l is the limiting conductivity of the suspension at low frequencies. This equation is derived from Eqs. (1) (2) (3) and (4) on the assumption that the conductivity of the plasmalemma is negligibly small compared with that of the external medium and the inner of cell, i.e., $\kappa_{mem} \ll \kappa_a, \kappa_p$ [38].

4. Results and discussion

4.1. Dielectric behavior of protoplast suspensions

The observed dielectric dispersion curves of protoplast suspensions with different concentrations were shown in Fig. 2, where the curves are the averaged results from three parallel samples. It can be seen that the dielectric dispersion occurred over the frequency range of 3 kHz–10 MHz, which was due to the interfacial polarization resulting from the build-up of charge at cell membrane when biological cells were placed in the electric field [13,17]. Compared with other curves in Fig. 2(b),

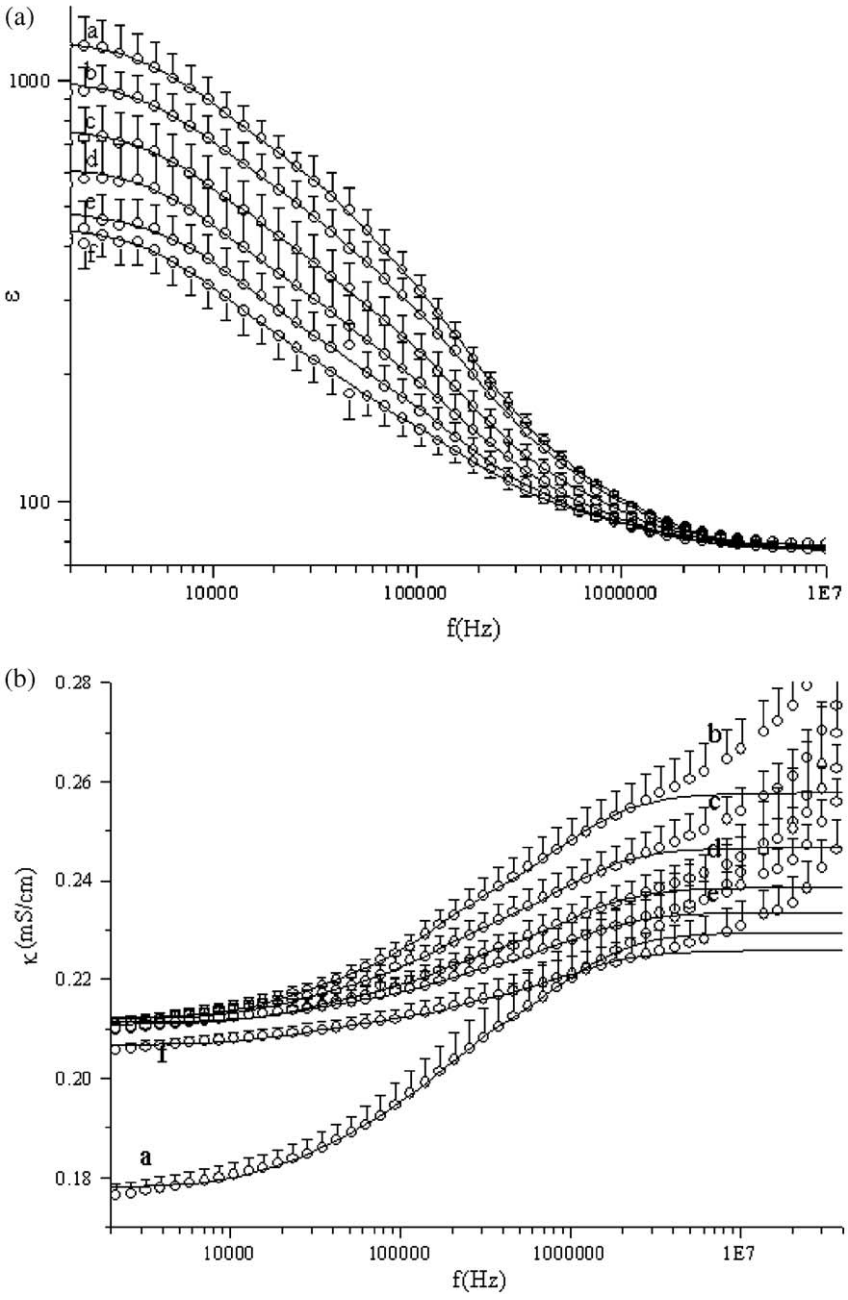

Fig. 2. Dielectric dispersion curves for the *Anabaena 7120* protoplast suspensions averaged from three parallel samples. Paired curves marked "a" refer to the most concentrated suspension and paired curves marked "f" to the most diluted suspension. Open circles are the data corrected for the electrode polarization effect. Solid lines depict the best fitted theoretical curves calculated Eq. (10) (four Debye-type terms) with the parameters listed in Table 3.

the depression of the limiting conductivity of the curve "a" (corresponding to the most concentrated suspension) at low frequencies may be because that the osmolarity between the cell and the suspending medium was not adjusted.

4.1.1. Comparison of several Cole–Cole dispersion equation fitting

To characterize the dielectric behavior of the protoplast suspensions, we firstly tried to fit the data by using a single Cole–Cole equation [39]:

$$\varepsilon^* = \varepsilon_h + \frac{\Delta\varepsilon}{1+(jf/f_0)^{1-\alpha}} + \frac{\kappa_l}{j2\pi f\varepsilon_v} \quad (7)$$

where $\Delta\varepsilon$ is magnitude of dielectric dispersion ($\Delta\varepsilon=\varepsilon_l-\varepsilon_h$), ε_l and ε_h are the limiting permittivity at low and high frequencies, respectively, f_0 characteristic frequency, κ_l the limiting conductivity at low frequencies, α the Cole–Cole parameter. The fitting results are summarized in Fig. 3 and Table 1.

It can be readily seen in Fig. 3 that a single Cole–Cole equation failed to fit the observed data over the frequency range. The deviation is reflected on the parameter α and the limiting dielectric parameters (ε_l, ε_h and κ_h, etc.). The value of α is a measure of the deviation of data from an ideal Debye-type dispersion given by the equation [40]:

$$\varepsilon^* = \varepsilon_h + \frac{\Delta\varepsilon}{1+jf/f_0} + \frac{\kappa_l}{j2\pi f\varepsilon_v}. \quad (8)$$

Apparently, the breadth of the dielectric dispersion as reflected by the value of α ($\alpha=0.34$) seemed to be too large. Such a large breadth of the β-dispersion cannot be merely explained in terms of the distribution of particle phase parameters (e.g., size) and is probably due to the overlapping of more two distinct sub-dispersions over the frequency range. And besides, the values of ε_h and κ_h also deviated visually from the experimental data. Therefore, we attempted to apply the Cole–Cole equation having two relaxation times (Eq. (9)) to fit the same data. The experimental curve was well simulated by using Eq. (9) with the best-fit parameters listed in Table 1. The Cole–Cole parameters of α ($\alpha_1=0.15$, $\alpha_2=0.13$) were smaller than 0.34. And the limiting dielectric parameters could also better agree with the observed values. This indicated that the dielectric spectra were truly composed of at least two sub-dispersions.

Table 1
Dielectric parameters obtained by means of Eqs. (7) and (9)

	ε_l	ε_m	ε_h	α_1	α_2	f_{01}	f_{02}	κ_l
Single Cole–Cole term	1400		64	0.34		0.018		0.178
Two Cole–Cole terms	1304	476	74	0.15	0.13	0.010	0.10	0.178

f in MHz, κ_l in mS/cm.

$$\varepsilon^* = \varepsilon_h + \frac{\Delta\varepsilon_1}{1+(jf/f_{01})^{1-\alpha_1}} + \frac{\Delta\varepsilon_2}{1+(jf/f_{02})^{1-\alpha_2}} + \frac{\kappa_l}{j2\pi f\varepsilon_v}. \quad (9)$$

4.1.2. Comparison of various Debye-type dispersion equations' fitting results

We attempted to use a sum of various Debye-type terms (Eq. (10)) to fit the same data in order to make certain how many sub-dispersions the investigated dielectric spectra consisted of. Here two, three and four Debye-type terms were employed to fit the same data, respectively. The fitting results were shown in Fig. 4(a) and the best-fit parameters were listed in Table 2.

$$\varepsilon^* = \varepsilon_h + \sum_{i=2,3,4}\frac{\Delta\varepsilon_i}{1+jf/f_{0i}} + \frac{\kappa_l}{j2\pi f\varepsilon_v}. \quad (10)$$

Obviously, there was a great discrepancy between the fitted curves using a sum of two, three Debye-type terms and

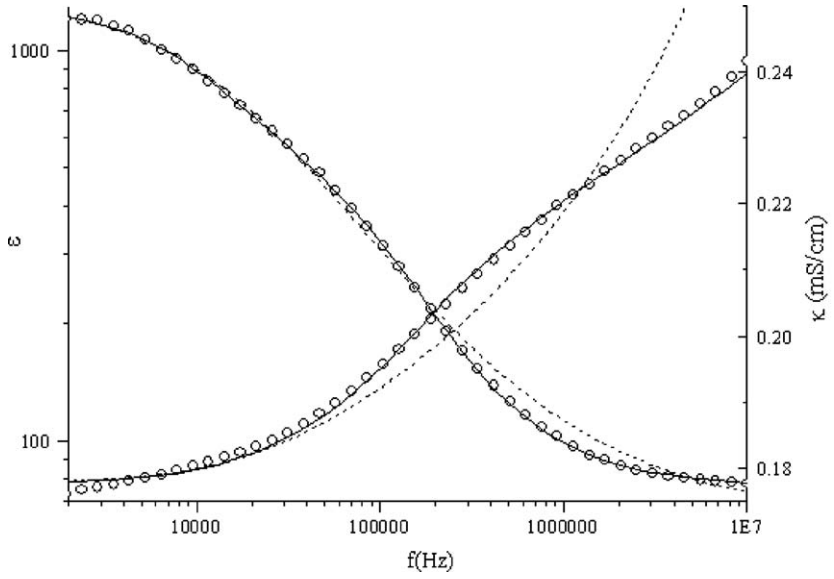

Fig. 3. The comparison of a single Cole–Cole equation and a sum of two Cole–Cole terms. Open circles are the data of the curve "a" in Fig. 2. Dashed lines depict the curve calculated from Eq. (7). Solid lines depict the curve calculated from Eq. (9). The parameters are listed in Table 1.

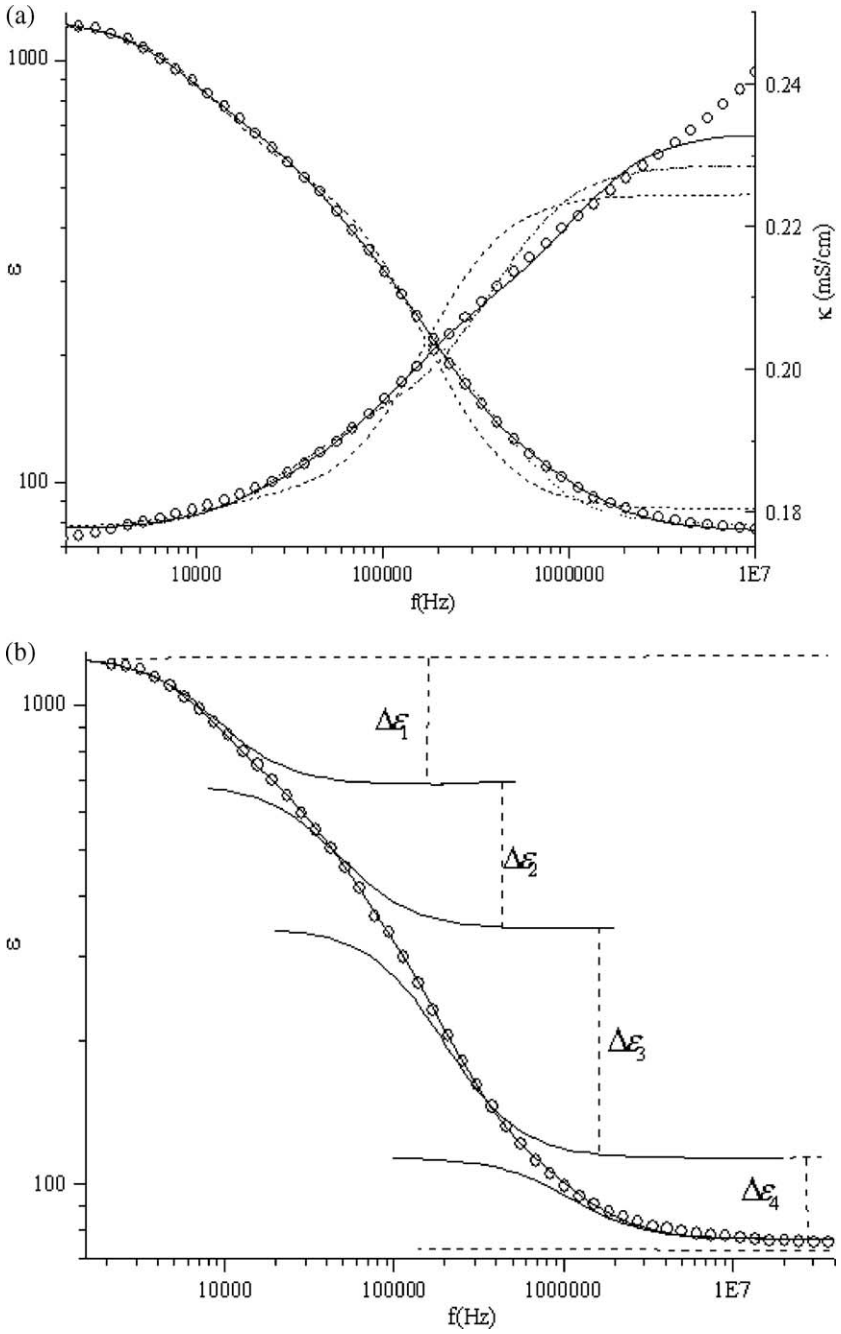

Fig. 4. (a) The comparison of two, three and four Debye-type terms. Open circles are the data of the curve "a" in Fig. 2. Dashed lines depict the curves calculated from Eq. (10) (i=2, i.e., two Debye-type terms). Dash-dotted lines depict the curves calculated from Eq. (10) (i=3, i.e., three Debye-type terms). Solid lines depict the best-fit curves calculated Eq. (10) (i=4, i.e., four Debye-type terms). The parameters are listed in Table 2. (b) The four distinct sub-dispersions separated from the whole dispersion of protoplast suspensions.

the observed dielectric spectra. However, the simulated curve using a sum of four Debye-type terms could satisfactorily agree with the experimental curve over the whole frequency range, and the limiting permittivity at low and high frequencies (ε_l and ε_h) were both consistent with the observed values (ε_l=1245, ε_h=76.8). Therefore, it was possibly inferred that the β-dispersion exhibited by *Anabaena* protoplast suspensions was a composite of at least four distinct sub-dispersions, and this may be the best interpretation of the large value of α. It is necessary to note that such behavior is characteristic for biological cells, especially for the cells containing intra-membranous structures [13,17,19,20,28,37,41]. For the sake of clarity, we separated these four distinct sub-dispersions from the whole dispersion and the results were shown in Fig. 4(b). Obviously, the whole dispersion was the overlapping of four distinct sub-dispersions. It can also be seen in Table 2 that the magnitude $\Delta\varepsilon_i$ of each sub-dispersion decreased with the increasing frequency, and the characteristic frequencies of two adjacent sub-dispersions were apart from roughly a decade order.

Table 2
Dielectric parameters obtained by means of Eq. (10)

	ε_l	$\Delta\varepsilon_1$	$\Delta\varepsilon_2$	$\Delta\varepsilon_3$	$\Delta\varepsilon_4$	ε_h	f_{01}	f_{02}	f_{03}	f_{04}	κ_l
Two Debye-type terms	1228	695	446			87	0.010	0.110			0.178
Three Debye-type terms	1250	607	413	151		79	0.008	0.055	0.302		0.178
Four Debye-type terms	1255	572	341	228	37	77	0.008	0.040	0.151	1.00	0.178

f in MHz, κ_l in mS/cm.

On the basis of the above analysis of dielectric behavior, all data in Fig. 2 were dealt with by using a sum of four Debye-type terms and the best-fit parameters were summarized in Table 3. For each sub-dispersion, the permittivity increment decreased as the decreasing protoplast concentration. This is expected because the mechanism of interfacial polarization depends on to a great extent the interfacial area, which is proportional to the number of particles dispersed in the suspension. In other words, the bigger the interfacial area is, the greater the degree of build-up of charge is, and the bigger the magnitude of dielectric dispersion is. On the other hand, the characteristic frequency f_{0i} of each sub-dispersion did not change remarkably within the range of protoplast concentration. This is also the characteristic of interfacial polarization.

In conclusion, the common characteristics of the four sub-dispersions may be summarized as: (a) the magnitude of the previous sub-dispersion is larger than that of the next sub-dispersion successively; (b) the characteristic frequency of the previous sub-dispersion is less than about one decade apart from the next one in turn.

4.2. Electrical phase parameters of protoplast components

Fig. 5 shows the experimental data and the theoretical curves simulated by single-shell model and the double-shell model as an example of curve (a) in Fig. 2. It can be readily seen that the theoretical curve simulated by the double-shell model gave a relatively satisfactory agreement with the experimental data than that simulated by the single-shell model, though there was some discrepancy at low frequencies possibly due to either the rough approximation of this model for the protoplast morphology or other factors. With regard to the disagreement at the high frequencies, it is possibly ascribed to two reasons: 1. the insufficient correction of stray inductance; 2. the dispersion caused by orientation polarization of the water or biological macromolecular in the protoplast at the high frequencies. When considering there is still no more realistic model to describe the lamella-distributed sheets of thylakoids at present, the double-shell model may be considered as a reasonable model to characterize it. At least, this model could give a plausible fitting for experimental data as a whole. In this way, all data in Fig. 2 were dealt with by the similar way, and all theoretical curves could agree with the experimental data from curve (b) to (f). The residuals are controlled in the range of (5.3±1.2)%. The estimated phase parameters were listed in Table 4.

Table 3
The dielectric parameters obtained through fitting a sum of four Debye-type terms to all the data in Fig. 2

	ε_l	$\Delta\varepsilon_1$	$\Delta\varepsilon_2$	$\Delta\varepsilon_3$	$\Delta\varepsilon_4$	f_{01}	f_{02}	f_{03}	f_{04}	κ_l
Dense	1255	572	341	228	37	0.008	0.040	0.15	1.00	0.178
	1005	446	259	190	33	0.008	0.038	0.16	1.02	0.212
	774	344	178	148	27	0.008	0.036	0.15	1.00	0.212
	624	294	140	93	21	0.009	0.044	0.18	1.06	0.211
	486	228	88	76	18	0.010	0.044	0.17	1.10	0.211
Dilute	448	215	88	54	13	0.009	0.043	0.20	1.25	0.207

f in MHz, κ_l in mS/cm.

The permittivity of plasmalemma ε_{mem} was estimated to be 6.5±0.5(if irrespective of 9.0), which was close to that of the plasmalemma reported by other researchers [28,30,41–43]. The value of 9.0 is relatively big possibly because of the errors of mathematic analysis when the magnitude of dielectric dispersion, especially that of conductivity, was very small.

The permittivity of the assumed equivalent shell of thylakoid ε_{thy} was estimated to be about 3.2±0.2, which is in the range of 1.5–9 for permittivity of various biological membranes reported [37,44–46]. If considering the thylakoid is composed of appressed membranes, then the estimated permittivity is understandable because it is actually the lamellate stack of two membranes [1]. Here this estimated value is only an apparent value and does not stand for the real value of thylakoid membrane. In addition, because of this uncertainty resulting from the rough approximation for this membranous apparatus, we should not discuss it in detail.

The permittivity of the cytoplasm (ε_{cyt}) and the nucleoplasmic region (ε_{nuc}) were estimated to be 60 and 100, respectively. It is possibly due to the difference between the cytoplasm and nucleoplasm. These two values (ε_{cyt} and ε_{nuc}) were sensitive to the limiting dielectric constant at the intermediate and high frequencies, respectively. Fig. 5 showed that the limiting permittivity at intermediate and high frequencies, calculated when $\varepsilon_{cyt}=60$ and $\varepsilon_{nuc}=100$, both agreed with the experimental data, which may suggested that the estimated values of ε_{cyt} and ε_{nuc} were relatively rational. The conductivity of the cytoplasm and the nucleoplasmic region were found to be 0.88±0.11 and 0.13±0.02 mS/cm, respectively. These two values were basically in the broad range from 0.4 to 5 mS/cm reported for the conductivity of the cytoplasm of various biological cells [28,30,46].

Next let us discuss the reason why there were at least four sub-dispersions. From the point of view of the M–W interfacial polarization theory [35], these protoplast components with different dielectric properties can produce four different kinds of interfaces amongst them (including the suspending medium, plasmalemma, cytoplasm, the equivalent

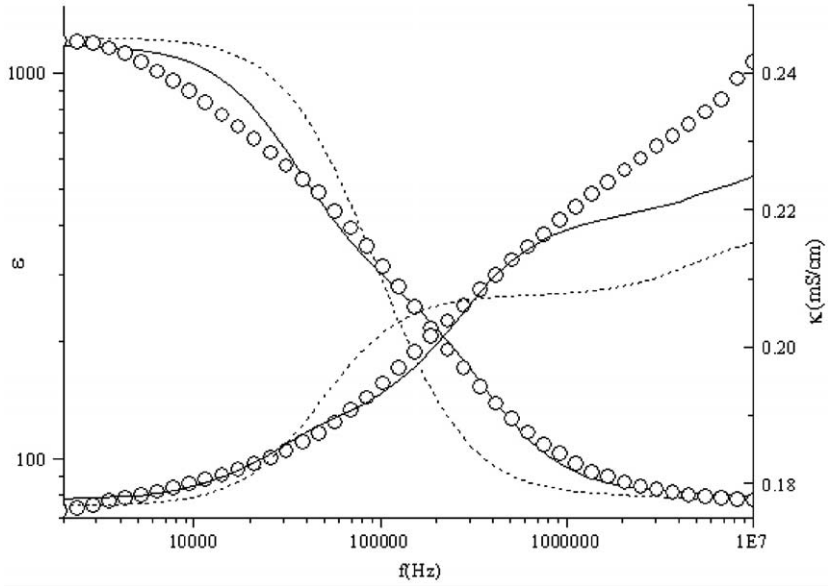

Fig. 5. Comparison between the experimental data (the curve a in Fig. 2) and the theoretical curve predicted by the double-shell model and the single-shell model. Solid lines: the theoretical curves predicted by the double-shell model. Dash lines: the theoretical curves predicted by the single-shell model. Related parameters: d_{mem}=7 nm, R=7 μm, R_{nuc}=2.9 μm, d_{thy}=14 nm, ε_{mem}=6.4, κ_{mem}=0, ε_a=78, κ_a=0.256 mS/cm, P=0.227, ε_{cyt}=60, κ_{cyt}=0.80 mS/cm, ε_{thy}=3.0, κ_{thy}=0.1 μS/cm, ε_{nuc}=100, κ_{nuc}=0.10 mS/cm.

shell of thylakoid and the nucleoplasm region), as shown in Fig. 1(c). Consequently, it may be reasonably thought that it was these four different kinds of interfaces that resulted in the four distinct sub-dispersions demonstrated in Section 4.1.2. At the same time, the characteristic frequencies of these four sub-dispersions were relatively near, which indicated that the four kinds of interfaces were possibly of similar properties, and this may explained why one dispersion, which appeared superficially a single dispersion, could be separated into four Debye-type sub-dispersions by the curve fitting.

5. Conclusions

The dielectric behavior exhibited by *Anabaena* protoplast suspensions was analyzed in detail and the conclusion was drawn that the observed dielectric spectra consisted of at least four Debye-type sub-dispersions over the frequency range from 0.01 to 10 MHz. The theoretical curve predicted by the double-shell model, in which an equivalent shell of thylakoid was assumed inside the protoplast, was employed to determine the dielectric properties of protoplast components. Here it is necessary to note that the double-shell model is only a rough approximation for the protoplast, and we expect a new, more appropriate model, which can accurately characterize the sheets of thylakoids distributed lamellarly in the protoplast, will be developed to further determine the real electric properties of protoplast components in vivo in the future. However, in any case, the present research could provide a sensitive sensor for judging the corresponding relationship between the inner structure (including its electric properties) and the characteristic parameters (such as the limiting permittivity at the low and high frequencies, etc) embodied by dielectric spectra of the protoplast suspensions.

Acknowledgement

This work is supported by the National Nature Science Foundation of China (No. 20273010).

Table 4
The estimated phase parameters in terms of the double-shell model

	κ_α (mS/cm)	P	ε_{mem}	ε_{cyt}	κ_{cyt} (mS/cm)	ε_{thy}	ε_{nuc}	κ_{nuc} (mS/cm)
a	0.256	0.227	6.4	60	0.80	3.0	100	0.10
b	0.267	0.147	7.0	60	1.00	3.5	100	0.15
c	0.250	0.107	7.1	60	1.00	3.5	100	0.15
d	0.246	0.100	6.1	60	0.80	3.0	100	0.12
e	0.237	0.076	6.0	60	0.80	3.0	100	0.12
f	0.220	0.040	9.0	60	1.00	4.0	100	0.25
$\bar{x}\pm$SD			6.5±0.5	60±0	0.88±0.11	3.2±0.3	100±0	0.13±0.02

Morphological parameters were: R=3 μm, d_{mem}=7 nm, d_{thy}=14 nm, R_{nuc}=2.9 μm, ε_α=78, κ_{thy}=0.1 μS/cm, κ_{mem}=0. Note: the value of $\bar{x}\pm$SD did not include the parameters estimated from curve (f). The residuals are controlled in the range of (5.3±1.2)%.

References

[1] P. Fay, The Blue-Greens: (Cyanophyta–Cyanobacteria), E. Arnold, London, 1983.
[2] D.G. Adams, Heterocyst formation in cyanobacteria, Curr. Opin. Microbiol. 3 (6) (2000) 618–624.
[3] G. Schmetterer, Cyanobacterial respiration, in: D.A. Bryant (Ed.), The Molecular Biology of Cyanobacteria, Kluwer Academic Publishers, Dordrecht, The Netherlands, 1994, pp. 409–435.
[4] S.I. Beale, Biosynthesis of cyanobacterial tetrapyrrole pigments: hemes, chlorophylls, phycobilins, in: D.A. Bryant (Ed.), The Molecular Biology of Cyanobacteria, Kluwer Academic Publishers, Dordrecht, 1994, pp. 519–558.
[5] A.Y. Semenov, M.D. Mamedov, S.K. Chamorovsky, Photoelectric studies of the transmembrane charge transfer reactions in photosystem ? pigment–protein complexes, FEBS Lett. 553 (2003) 223–228.
[6] A. Agostiano, M. Caselli, Phetoelectrochemistry of thylakoid membranes, Bioelectrochem. Bioenerg. 42 (1997) 255–262.
[7] L.I. Krishtalik, Fast electron transfers in photosynthesis reaction center: effect of the time-evolution of dielectric response, Biochim. Biophys. Acta 1228 (1995) 58–66.
[8] A.H. Elcock, J.A. McCammon, Electrostatic contributions to the stability of halophilic proteins, J. Mol. Biol. 280 (1998) 731–748.
[9] A.M. Kuznetsov, J. Ulstrup, Fluctuational tunnel effects and vibrational dispersion in primary electron transfer processes of bacterial photosynthesis, Spectrochim. Acta Part A 54 (1998) 1201–1209.
[10] U. Zimmermann, W.M. Arnold, in: H. Fröhlich, F. Kremer (Eds.), Coherent Excitations in Biological Systems, Springer-Verlag, Berlin, 1983, pp. 211–221.
[11] R. Pethig, D.B. Kell, The passive electrical properties of biological systems: their significance in physiology, biophysics and biotechnology, Phys. Med. Biol. 32 (1987) 933–970.
[12] S. Takashima, Electrical Properties of Biopolymers and Membranes, Adam Hilger, Bristol, 1989.
[13] K.R. Foster, H.P. Schwan, in: C. Polk, E. Postow (Eds.), Handbook of Biological Effects of Electromagnetic Fields, Second edition, CRC Press, 1996, pp. 27–106.
[14] C.M. Mihai, M. Mehedintu, E. Gheorghiu, The derivation of cellular properties from dielectric spectroscopy data, Bioelectrochem. Bioenerg. 40 (1996) 187–192.
[15] G.H. Markx, C.L. Davey, The dielectric properties of biological cells at radio frequencies: applications in biotechnology, Enzyme Microb. Technol. 25 (1999) 161–171.
[16] J. Gimsa, Characterization of particles and biological cells by AC Electrokinetics, in: A.V. Delgado (Ed.), Interfacial Electrokinetics and Electrophoresis, Marcel Dekker Inc., New York, 2001, pp. 369–400.
[17] K. Asami, Characterization of heterogeneous systems by dielectric spectroscopy, Prog. Polym. Sci. 27 (2002) 1617–1659.
[18] Y. Feldman, I. Ermolina, Y. Hayashi, Time domain dielectric spectroscopy study of biological systems, IEEE Trans. Dielectr. Electr. Insul. 10 (5) (October 2003) 728–753.
[19] V. Raicu, T. Saibara, A. Irimajiri, Dielectric properties of rat liver in vivo: a noninvasive approach using an open-ended coaxial probe at audio/radio frequencies, Bioelectrochem. Bioenerg. 47 (1998) 325–332.
[20] V. Raicu, T. Saibara, H. Enzan, A. Irimajiri, Dielectric properties of rat liver in vivo: analysis by modeling hepatocytes in the tissue architecture, Bioelectrochem. Bioenerg. 47 (1998) 333–342.
[21] H. Fricke, The electrical capacity of suspensions with special reference to blood, J. Gen. Physiol. 9 (1925) 137–152.
[22] W.M. Arnold, U. Zimmermann, Rotating-field-induced rotation and measurement of the membrane capacitance of single mesophyll cells of *Avena sativa*, Z. Naturforsch. 37c (1982) 908–915.
[23] G. Fuhr, J. Gimsa, R. Glaser, Interpretation of electro rotation of protoplasts: I. Theoretical considerations, Stud. Biophys. 108 (1985) 149–164.
[24] J. Gimsa, G. Fuhr, R. Glaser, Interpretation of electro rotation of protoplasts: II. Interpretation of experiments, Stud. Biophys. 109 (1985) 5–14.
[25] R. Glaser, G. Fuhr, J. Gimsa, Rotation of erythrocytes, plant cells and protoplasts in an outside rotating electric field, Stud. Biophys. 96 (1983) 11–20.
[26] R.V.E. Lovelace, D.G. Stout, P.I. Steponkus, Protoplast rotation in a rotating electric field: the influence of cold acclimation, J. Membr. Biol. 82 (1984) 157–166.
[27] K.V.I.S. Kaler, T.B. Jones, Dielectrophoretic spectra of single cells determined by feedback-controlled levitation, Biophys. J. 57 (1990) 173–182.
[28] K. Asami, T. Yamaguchi, Dielectric spectroscopy of plant protoplasts, Biophys. J. 63 (1992) 1493–1499.
[29] R.Y. Stanier, R. Kunisawa, M. Mandel, G. Cohen-Bazire, Purification and properties of unicellular blue-green algae (Order Chroococcales), Bacteriol. Rev. 35 (1971) 171–205.
[30] K. Asami, Dielectric properties of protoplasm, plasma membrane and cell wall in yeast cells, Bull. Inst. Chem. Res., Kyoto Univ. 55 (4) (1977) 394–414.
[31] K. Asami, A. Irimajiri, T. Hanai, N. Shiraishi, K. Utsumi, Dielectric analysis of mitochondria isolated from rat liver. I. Swollen mitoplasts as simulated by a single-shell model, Biochim. Biophys. Acta 778 (1984) 559–569.
[32] A. Irimajiri, T. Hanai, A. Inouye, A dielectric theory of "multi-stratified shell" model with its application to a lymphoma cell, J. Theor. Biol. 78 (1979) 251–269.
[33] J.C. Maxwell, A Treatise on Electricity and Magnetism, Clarendon Press, Oxford, 1891. 3rd.
[34] K.W. Wagner, Erklärung der dielectrischen Nachwirkungsvorgänge auf Grund Maxwellscher Vorstellungen, Arch. Electrotech. 2 (1914) 371–387.
[35] T. Hanai, H.Z. Zhang, K. Sekine, K. Asaka, K. Asami, The number of interfaces and the associated dielectric relaxations in heterogeneous systems, Ferroelectrics 86 (1988) 191–204.
[36] C.L. Davey, H.M. Davey, D.B. Kell, On the dielectric properties of cell suspensions at high volume fractions, Bioelectrochem. Bioenerg. 28 (1992) 319–330.
[37] V. Raicu, G. Raicu, G. Turcu, Dielectric properties of yeast cells as simulated by the two-shell model, Biochim. Biophys. Acta 1274 (1996) 143–148.
[38] H. Pauly, H.P. Schwan, Uber die impedanz einer suspension von kugelformigen eilchen mit einer schale, Z. Naturforsch. 14b (1959) 125–131.
[39] K.S. Cole, R.H. Cole, Dispersion and absorption in dielectrics. ?. Alternating current characteristics, J. Chem. Phys. 9 (1941) 341–351.
[40] P. Debye, Polar Molecules, Dover Publications, New York, 1945.
[41] K. Asami, T. Yonezawa, Dielectric behavior of wild-type yeast and vacuole-deficient mutant over a frequency range of 10 kHz to 10 GHz, Biophys. J. 71 (1996) 2192–2200.
[42] H.P. Schwan, Electrical properties of tissue and cell suspensions, in: J.H. Lawrence, C.A. Tobias (Eds.), Advances in Biological and Medical Physics, vol. 5, Academic Press, New York, 1957, pp. 147–209.
[43] J. Gimsa, R. Glaser, G. Fuhr, in: W. Schütt, H. Klinkmann, I. Lamprecht, T. Wilson (Eds.), Physical Characterization of Biological Cells, Verlag Gesundheitt, Berlin, 1991, pp. 295–323.
[44] F. Bordi, C. Cametti, T. Gili, Dielectric spectroscopy of erythrocyte cell suspensions. A comparison between Looyenga and Maxwell–Wagner–Hanai effective medium theory formulations, J. Non-Cryst. Solids 305 (2002) 278–284.
[45] J. Gimsa, T. Muller, T. Schnelle, G. Fuhr, Dielectric spectroscopy of single human erythrocytes at physiological ionic strength: dispersion of the cytoplasm, Biophys. J. 71 (1996) 495–506.
[46] R. Hölzel, Non-invasive determination of bacterial single cell properties by electro rotation, Biochim. Biophys. Acta 1450 (1999) 53–60.